



Missouri University of Science and Technology
Scholars' Mine

Materials Science and Engineering Faculty
Research & Creative Works

Materials Science and Engineering

01 Jun 1998

Mixed Electron Emission from Lead Zirconate-Titanate Ceramics

Weiming Zhang

Wayne Huebner

Missouri University of Science and Technology, huebner@mst.edu

Stephen E. Sampayan

Mike L. Krogh

Follow this and additional works at: https://scholarsmine.mst.edu/matsci_eng_facwork

 Part of the [Materials Science and Engineering Commons](#)

Recommended Citation

W. Zhang et al., "Mixed Electron Emission from Lead Zirconate-Titanate Ceramics," *Journal of Applied Physics*, vol. 83, no. 11, pp. 6055-6060, American Institute of Physics (AIP), Jun 1998.

The definitive version is available at <https://doi.org/10.1063/1.367474>

This Article - Journal is brought to you for free and open access by Scholars' Mine. It has been accepted for inclusion in Materials Science and Engineering Faculty Research & Creative Works by an authorized administrator of Scholars' Mine. This work is protected by U. S. Copyright Law. Unauthorized use including reproduction for redistribution requires the permission of the copyright holder. For more information, please contact scholarsmine@mst.edu.

Mixed electron emission from lead zirconate–titanate ceramics

Weiming Zhang^{a)} and Wayne Huebner

The Department of Ceramic Engineering, University of Missouri-Rolla, Rolla, Missouri 65401

Stephen E. Sampayan

University of California, Lawrence Livermore National Laboratory, Livermore, California 94551

Mike L. Krogh

Allied Signal Federal Manufacturing & Technologies,^{b)} Kansas City, Missouri 64141

(Received 12 December 1997; accepted for publication 27 February 1998)

Simultaneous ferroelectric and plasma emission from $\text{Pb}(\text{Zr,Ti})\text{O}_3$ was observed with only a negative driving pulse applied to the sample, and without an extraction potential on the electron collector. Plasma emission was a strong, inconsistent, and self-destructive process. In addition, a positive ion current was detected. Comparatively, ferroelectric emission was a relatively stable self-emission process, exhibiting no apparent delay time, and no positive ion current. The relationship between the switching and emission current of ferroelectric samples measured simultaneously cannot only be used to determine the existence of ferroelectric emission, but can also give direction to choosing suitable ferroelectric materials for emitter applications. © 1998 American Institute of Physics. [S0021-8979(98)03911-5]

I. INTRODUCTION

Strong electron emission (J_c as high as 100 A/cm^2) from ferroelectrics due to fast polarization switching [i.e., ferroelectric emission, (FE)] was discovered at CERN in 1988.¹ Research activities quickly spread around the world, triggered by applications in the field of accelerator technology, and especially possible applications in microelectronic devices such as flat panel displays.^{1–3} However, a diverse array of results and explanations concerning FE have appeared, leading to uncertainties in understanding underlying mechanisms.

Most studies have utilized disk-shaped ferroelectrics with Au or Ag grid electrodes at the emitting surface. At the opposite side a solid electrode (applied with a driving field) has been used. The commonly accepted principle of FE is that a ferroelectric material appropriately polarized will have the positive charges of the dipoles oriented towards the ferroelectric surface between the grid electrodes. The resulting net positive charge on the surface is compensated by electrons in order to preserve charge neutrality. Upon fast reversal of the polarization, the negative charges of the ferroelectric dipoles orient towards the surface, leading to a rapid buildup of a repulsive electrostatic force.^{1–7} This field has been modeled to be as high as 3×10^8 to 10^9 V/m .^{7–9} However, this principle cannot explain the following phenomena convincingly:

- (1) The electron emission intensity increases with temperature, and occurs far above the Curie temperature (i.e., at temperature where no spontaneous polarization exists);^{5,10–13}
- (2) Published emission current densities as high as

10^5 A/cm^2 are far beyond what the value of spontaneous polarization of ferroelectrics (at most $100 \mu\text{C/cm}^2$) can contribute;¹³

- (3) No direct experimental evidence has shown that the electrons are emitted from the bare surface of the ferroelectric during polarization switching.

A “plasma emission mode” has been presented, which ascribes these effects to the creation of a surface discharge plasma.^{13–15} However, this mode of emission damages the ceramic surface after only a few minutes of operation.¹³ This is detrimental for reliable application or fundamental measurements. In addition, one should note that the experimental techniques varied widely among these research groups. A negative pulse with a fast risetime (tens of ns) and short pulse width (few hundred ns) are the conditions believed to result in “true” ferroelectric emission.^{16,17} No extraction field was applied to the electron collector. However, negative pulses with a slower pulse risetime (few hundred ns) and longer pulse width (few μs) were also used to induce ferroelectric emission by the same research group in earlier published studies^{10,11} as well as other research groups.^{5,6,18} It was also mentioned that luminosity does not appear to correspond with emission current with or without an extraction field.¹⁹ Comparatively, a high positive extraction potential on the electron collector results in a plasma emission mode;^{13–15} under this condition the Child–Langmuir law applies. In addition, different electrode configurations have been used, including sputtered Au^{10–12,16–18} and copper wire grids simply pressed onto the surface.^{13,15,19}

Thus, a better understanding of this complex emission process is necessary, not only for successful applications but also for theoretical reasons. In this work both types of electron emission process were simultaneously observed.

II. EXPERIMENTAL TECHNIQUES

Disk-shaped samples ($\Theta = 19 \text{ mm}$; $t = 0.64 \text{ mm}$) of a commercially available $\text{Pb}(\text{Zr,Ti})\text{O}_3$ (PZT) EC-64 (EDO Co.,

^{a)}Corresponding author: Electronic mail: weiming@umr.edu

^{b)}Operated for the United States DOE under Contract No. DE-AC04-DP00613. Copyright Allied Signal Inc., 1998.

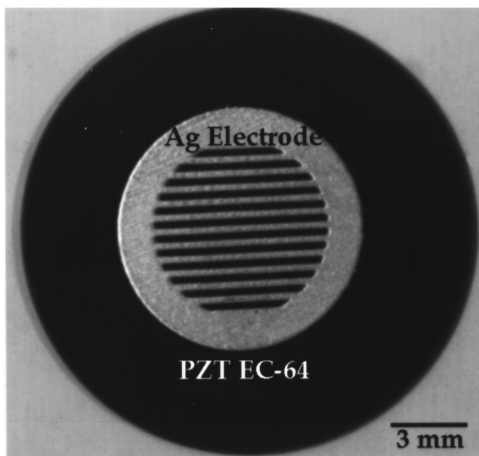


FIG. 1. Ferroelectric emitter surface pattern showing grid electrode with $\Theta \approx 9$ mm and grid width ≈ 300 μm .

Utah), were prepared using a conventional ceramic processing.²⁰ Surface were polished with 300 grit SiC paper, and then ultrasonically cleaned in acetone. Screen-printed Ag electrodes ($\Theta \approx 9.5$ mm) were applied; fully solid on the rear side and a grid on the other side. Interconnected stripe electrodes were 300 μm wide, and 300 μm apart (see Fig. 1). Samples were fired at $780^\circ\text{C} \times 0.5$ h to improve the electrode adhesion, and then were glued onto a 9.5-mm-diam copper rod using silver paste. The copper ground connection on the grid electrode side was also electrically attached with silver paste. Samples were heat treated in a furnace at 200°C for 12 h to eliminate any outgassing of the silver paste. This step is important, as any residual gas in the paste will induce a strong discharge.

Figure 2 shows a schematic diagram of the experimental setup. Ferroelectric samples were set in the vacuum chamber with the grid electrode side facing the electron collector (a flat Pt foil). The collector area was at least 1.5 times larger than the emission area. The distance between the sample and electron collector was set at ≈ 4 or 5 mm. The electron collector can be either kept at the same potential as grid electrode (i.e., no extraction potential between ferroelectric ma-

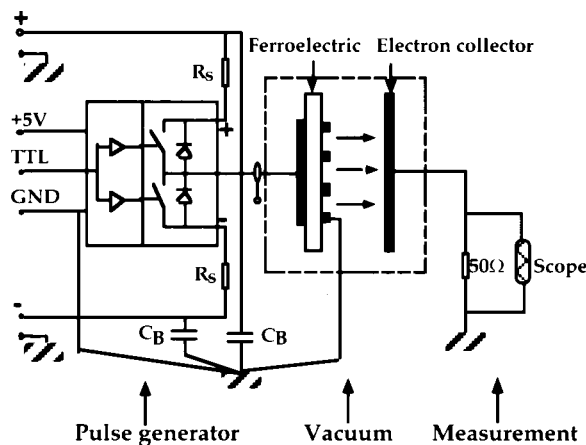


FIG. 2. Schematic diagram of the experimental setup. $R_s = 35\text{--}100$ Ω , $C_B = 10\text{--}20$ nF.

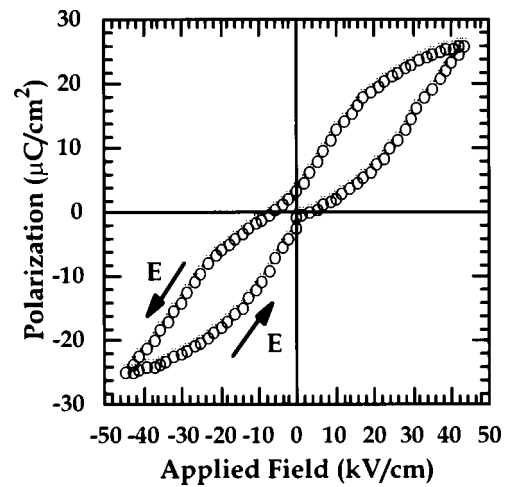


FIG. 3. Hysteresis loop of PZT EC-64 with grid electrodes at room temperature.

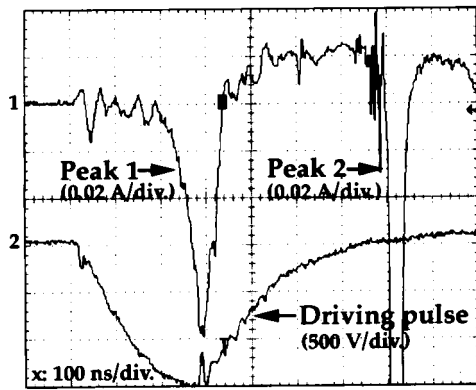
terial and collector), or a positive or negative potential up to 1500 V can be applied. Driving pulses were input to the rear electrode of sample, while the grid electrode was kept at the ground state. The pulse generator is comprised of one fast high voltage switch (HTS 31-GSM, Eurotek Inc. NJ), two dc power supplies (APH2000M, KEPCC Co., NY), and one pulse function generator (Model 81, Wavetek Co., CA). This combination can generate high voltage (≤ 3 kV), unipolar or bipolar pulses with a fast rise time (≤ 300 ns/3 kV) and adjustable pulse width (≥ 200 ns). In order to minimize electrical noise, all connector cables were shielded and runs made as short as possible.

A cable with a 50 Ω impedance was soldered on the electron collector and connected to a measurement circuit. Collected emission electrons flow through a 50 Ω resistor; a digital real time oscilloscope (TDS 380, Tektronix Co., OR) with 400 MHz bandwidth was used to measure the voltage drop. The charging and switching current was measured using a current probe (TM 502A, Tektronix Co., OR) with 50 MHz bandwidth. All studies were performed in a vacuum of $10^{-6}\text{--}10^{-8}$ Torr.

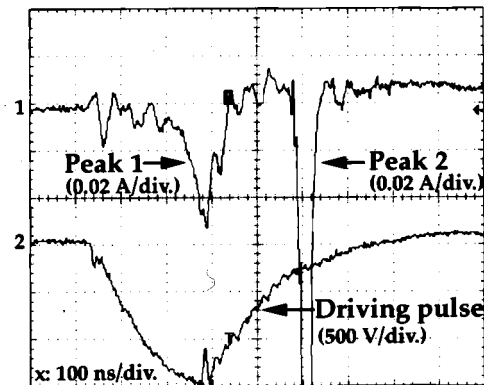
Hysteresis loops of samples with grid electrodes were measured using a ferroelectric material testing system (RT6000, Radiant Technologies, Inc., NM). The capacitance of samples were ≈ 1.1 nF. Samples were prepoled prior to emission studies by applying a dc electric field of 31 kV/cm with the negative polarity on the grid electrode at room temperature in the vacuum chamber for 2 h.

III. RESULTS AND DISCUSSION

The switching characteristics at a ferroelectric can be partially evaluated from the hysteretic behavior. Figure 3 exhibits the hysteresis loop for the PZT sample. This is classic “pinched loop” behavior, indicative of the “hardness” of the PZT. That is, at room temperature, the strain energy of 90° domain reversal cannot be totally overcome, hence saturation of the loop is not achieved for even a bias field of 45 kV/cm, and the remanent polarization P_r is low. In this case $P_r \approx 4$ $\mu\text{C}/\text{cm}^2$.



(a)



(b)

FIG. 4. Typical emission current traces when a negative driving pulse is applied to the sample and with no extraction potential on the collector (two consecutive recordings).

Typical emission results with only a negative driving pulse applied to the sample and without an extraction potential on the electron collector are shown in Figs. 4(a) and 4(b). One should note that these results are different compared to the results of other groups who reported true ferroelectric emission^{1,4,5,6,11,16,18} or plasma emission.^{13–15} Most studies have shown only one emission peak per driving pulse. However, our results showed two clearly distinguishable emission peaks per driving pulse. Peak 2 always occurred anywhere from 200 to 500 ns after peak 1, and always had a higher amplitude than peak 1. Peak 2 also varied in magnitude (0.2–1 A) during repeated measurements. Comparatively, the position of peak 1 was relatively stable, i.e., almost no delay time. Note that Figs. 4(a) and 4(b) are two consecutive recordings.

Initially these emission results were interpreted as true ferroelectric emission, as the basic conditions of ferroelectric emission were met, such as a negative and relatively fast driving pulse with short pulse duration, and no extraction potential on the electron collector. Thus according to the principle of the true ferroelectric emission, no emission peak should be exhibited if only a positive driving pulse is applied to the rear electrode of the sample: the positive charge of the

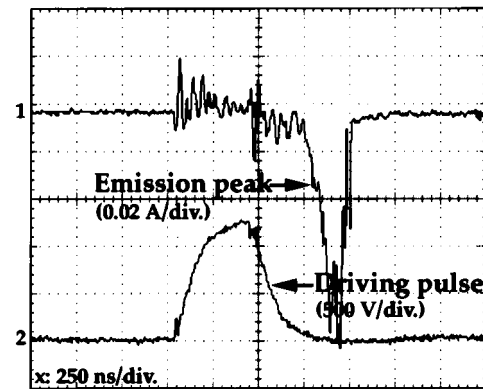


FIG. 5. The emission current trace when a positive driving pulse is applied.

dipoles will orient to the grid electrode side of the sample, representing an attractive rather than repulsive electrostatic force on electrons present on the ferroelectric surface. Nevertheless, Fig. 5 shows the results under positive pulse conditions; one strong emission peak was still observed, and the peak amplitude and time position were unstable.

Comparing the peak position of Figs. 4 and 5, it is clear that emission peak 2 in Fig. 4 is still present. Both emission peaks have an apparent delay time (200 ns–500 ns) from the full amplitude of the applied pulse. This apparent delay time, insensitivity to driving pulse polarity, and instability are characteristics of plasma emission.

A plasma has a typical expansion velocity of ≈ 2 cm/ μ s in a vacuum,^{13,21} which does not have a strong dependence upon the cathode material. Thus, provided that the plasma forms on the sample surface when the driving pulse reaches its maximum, then the delay time to the collector can be calculated. In this experiment, the distance between the sample and electron collector was ≈ 5 mm, which corresponds to a transit time of ≈ 250 ns. This calculated delay time matches Figs. 4 and 5 quite well.

The observed inconsistency is a common and important characteristic of a plasma. The behavior of plasma is governed by collective effects due to electromagnetic interaction among the charged particles and the particle's instability determines the plasma inconsistency in terms of uncertainty of state and motion. Many mechanisms can produce the inconsistency of a plasma, such as collision induced instability, ionization instability, rotation induced instability, and pressure driven instability etc.²² Any of these instabilities will change the local charge density, local charge expansion velocity etc., which in turn leads to the inconsistency of the time position and amplitude of the current emission peak.

A plasma is usually defined as an ionized gas in a state of electrical "quasineutrality." However, charge excess plasmas also exist, in which there is an excess in the number per unit volume of the positive or negative particles (ion or electron excess plasma).^{22,23} No matter which case, positive ions exist in a plasma. Thus, in order to confirm the presence of plasma emission, a strong negative extraction field (-2.5 kV/cm) was applied to the electron collector to see if a positive peak could be detected. Figure 6 is a typical result. The detected positive peak can only be due to the collection

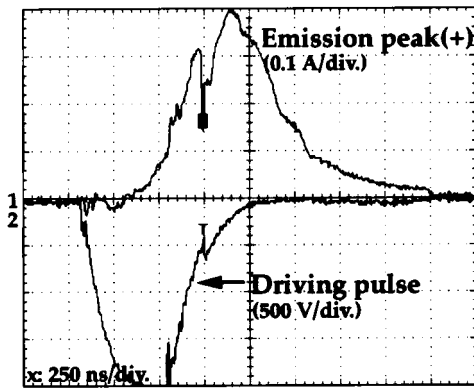


FIG. 6. The detected ion current when -1000 V is applied to the electron collector.

of ions. The maximum of the broad positive peak is delayed ≈ 350 ns from the driving pulse, which matches that of peak 2 in Fig. 4. However, the positive emission current and charge are much stronger than the electron emission shown in Fig. 4, which is due to the applied high extraction field to the collector in this experiment. These results suggest a conclusion that peak 2 of the emission process shown in Fig. 4 is due to plasma emission.

The plasma was most likely induced from the metal-dielectric-vacuum triple gaps at the edge of Ag grid electrode. The scanning electron microscopy (SEM) micrograph shown in Fig. 7 of a sample polished cross section prior to emission shows the presence of small gaps that are microns in size. These gaps are due to imperfect adhesion between electrode and ceramic, especially at the edge of the electrode. The enhancement of the electric field in these gaps, E_g , is given by:^{13,15,24}

$$E_g \approx KE_a, \quad (1)$$

where K is the dielectric constant of material and E_a is the driving electric field.

Since the dielectric constant for PZT EC-64 is ≈ 1300 (25°C , 1 kHz), and $E_a \approx 31$ kV/cm, so $E_g = 4 \times 10^9$ V/m.

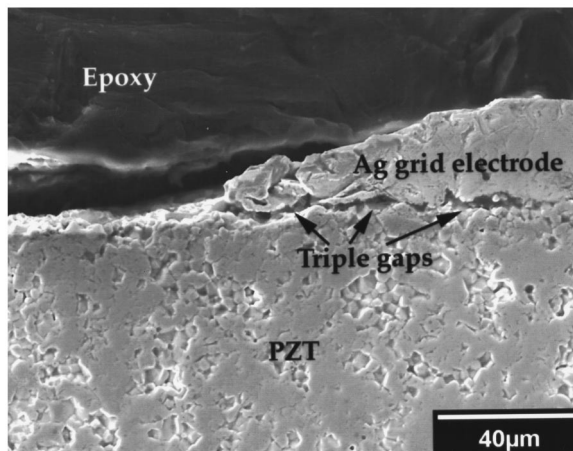


FIG. 7. SEM micrograph of sample polished cross section showing the triple gaps between the ceramic and the grid electrode.

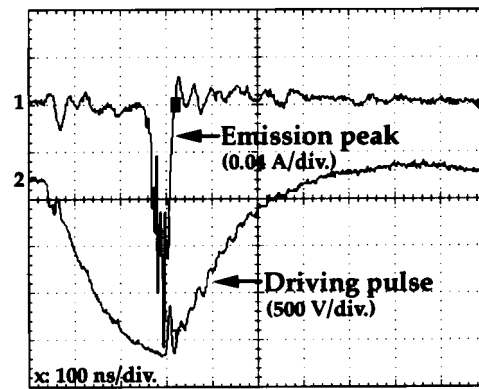


FIG. 8. A typical emission current trace for a 250 Hz driving pulse without extraction field.

Under this high electric field, classic field electron emission from the triple points will undoubtedly occur. This is known as “prebreakdown” field emission if the gap is seen as a classical diode. The Ag grid electrode and ceramic surface serve as a cathode or anode, respectively, depending on the polarity of the driving field. The breakdown of this gap can be either cathode or anode initiated. The Ag electrode plays a critical role because of its low melting point. When a positive field is applied, the Ag electrode served as a cathode, the field emission current flowing through a point on the electrode causes it to heat up. Subsequently it melts and vaporizes, thus in the end leading to breakdown.

When a negative field is applied, the grid electrode serves as an anode. Yet breakdown can also be initiated by electrons accelerated across the vacuum gap which impact on a section of the Ag surface, causing it to heat and vaporize. These effects are the reason that the observed plasma emission was not sensitive to the driving field polarity. As vapor fills the gap, ions form and electron avalanche occurs, consequently the gap conductance increases and the discharge changes into an arc.

Other evidence of this kind of plasma formation was found from SEM micrographs of the emission surface.²⁵ However, plasma formation on the emission surface might be much more complicated than we have hypothesized. Other possible sources for plasma formation is the locally high electric fields associated with different domain orientations near the surface. With the existing experimental system, alternate mechanisms such as this could not be explored.

However, the position and amplitude of emission peak 1 in Fig. 4 are clearly quite different with that of emission peak 2. The position and amplitude of peak 1 are relatively steady. Thus, it is certain that peak 1 corresponds to a different emission mode. When the driving pulse frequency was increased above 200 Hz, peak 2 in Fig. 4 totally disappeared, and only peak 1 appeared (Fig. 8). Kofoid²⁴ also observed that plasma emission was more likely to occur at low frequencies. However, the reason is not clear. Increasing the frequency of the driving pulse also decreased the width of the emission peak, although the integrated current density was greater.

The same negative field (-2.5 kV/cm) was applied to

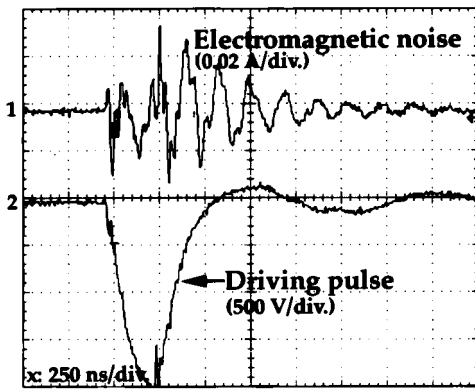


FIG. 9. A typical emission result for a high frequency (250 Hz) driving pulse with -1000 V applied to the electron collector.

the electron collector to see if the emission at 250 Hz contained a positive ion current. The results, shown in Fig. 9, yielded just electromagnetic noise, i.e., no positive ions were detected. Note that the electromagnetic noise was also observed in the other experiments of Figs. 4–6 and 8, however, the noise level is lower, as no field was biased on the collector (for Figs. 4–6), and the noise could also be suppressed by the emission signal. The noise exhibits some periodicity, with a frequency of 6 MHz. This noise may be due to piezoelectric “ringing.” For this sample, the fundamental thickness mode resonance would occur at ≈ 3 MHz (calculated by N_f/d ; N_f : frequency constant ≈ 2026 Hz m, d : sample thickness $\approx 6.4 \times 10^{-4}$ m.) The absence of a negative peak is due to the strong negative potential on electron collector which repels the emission electrons, and from which the energy of emission electron is predicted to be under 1000 eV. From this result, we conclude that the emission peak 1 in Fig. 4 corresponds to true ferroelectric emission.

More direct evidence was obtained by measuring the charging current (due to the sample capacitance) and switching current (due to the polarization or domain switching), as

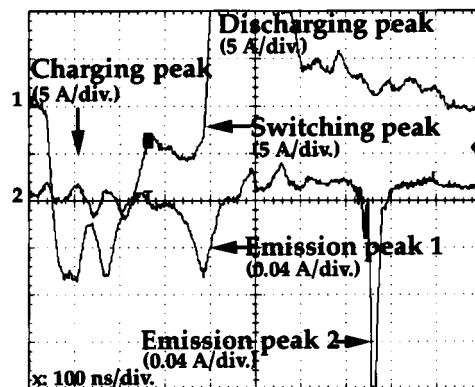


FIG. 10. The time corresponding relationship between switching and emission current with a -2000 V driving pulse applied to sample and without extraction potential on the collector.

well as the emission current simultaneously as shown in Fig. 10. The inversion “double hump” recorded in channel 1 mostly represents charging current, as ferroelectrics initially behave like a linear dielectric (i.e., simple capacitor). However due to the relatively large RC time, the charging current and the switching current overlap. The switching current is always late to charging current, as domain or polarization switching is relatively slower than the ionic and electronic polarization, and only occurs when driving field reaches the threshold values. From the integrated current, the total charge of this inversion double hump peak is $2.88 \mu\text{C}$, while the charge necessary to load the linear dielectric part of the sample to 2000 V (driving voltage) is $1.98 \mu\text{C}$ (calculated from $Q = C \times V$). So the excess charge $2.88 - 1.98 = 0.90 \mu\text{C}$ is due to the polarization switching. The second peak, which also represents the switching current, corresponds to $0.5 \mu\text{C}$, thus the total switching charge under this circumstance is $\approx 1.4 \mu\text{C}$ ($\approx 2.54 \mu\text{C}/\text{cm}^2$, calculated from the electrode area $\approx 0.55 \text{cm}^2$). This corresponds to switching $\approx 10\%$ of the total polarization ($P_m \approx 25 \mu\text{C}/\text{cm}^2$ from Fig. 3). The switching process lasts ≈ 150 ns, then cuts off by the discharging peak. The time corresponding relationship between the switching current and emission current peak 1 gives a strong evidence that the emission peak 1 is induced by the dipolar or domain switching in the sample. There is a ≈ 40 ns delay between the maximum of the switching peak and the emission peak 1. Note, no switching peak corresponds to emission peak 2.

From these results, we conclude that the emission current peak 1 is due to the true ferroelectric emission, as it satisfies three main criteria: (1) self-emission (no extraction field applied to electron collector),^{1,17} (2) no ion current detected,¹⁹ and (3) corresponds to the domain switching.^{4,17}

From the integrated emission current peak 1 in Fig. 10, it turns out that just 4 nC was emitted, which corresponds to only 0.3% of the switched charge ($\approx 1.4 \mu\text{C}$). This low FE efficiency is probably due to the slow rise time of the driving pulse (≈ 2000 V/200 ns), thus some charges can flow away through the surface or bulk of the sample. Also some charges are probably captured by the plasma and thus contribute to the plasma emission peak. Again note that the plasma emission current was much higher than FE emission current in either Fig. 4 or 10. Another reason for the low FE current is the inherent hardness of PZT EC-64. The hysteresis loop shown in Fig. 3 reflects that it cannot be saturated even for a driving field as high as 45 kV/cm. For most of the emission experiments, the applied field was ≈ 31 kV/cm, thus the domain switching percentage was quite low, as confirmed from the switching current plot (Fig. 10). Thus the repulsive electrostatic force induced on the ferroelectric surface will also be low.

The observed fact that almost no delay time exists for emission peak 1 can be explained as follows:²⁶ Miller *et al.*⁸ calculated that for BaTiO₃ single crystal the repulsive field strength E on the surface layer due to polarization switching would range from 3×10^8 to 10^9 V/m. This calculation was based on the hypothetical existence of a low dielectric constant ($K \approx 10$ –100) surface layer and full polarization switching. Although for PZT and PLZT materials the exist-

tence of this surface layer has not yet been proven,²⁷ due to the many similarities to BaTiO₃²⁸ it is reasonable to assume that the result of Miller *et al.* also fits the PZT case. However, in this experiment, only 10% of the spontaneous polarization ($2.54 \mu\text{C}/\text{cm}^2$) was switched. Thus, it is more reasonable to decrease the field strength to 10%. Hence, E would be $3 \times 10^7 \text{ V/m}$.

Provided that the electrons are located on the surface, then the force on an electron would be:

$$F = eE = 4.8 \times 10^{-12} \text{ CV/m} \quad (2)$$

then the acceleration of electrons would be:

$$a_x = \frac{F}{m} = 5.3 \times 10^{18} \text{ CV/mk g} \quad (3)$$

so:

$$Z = V_0 t + \frac{1}{2} a_x t^2, \quad (4)$$

where Z is the distance between the emission surface and collector ($5 \times 10^{-3} \text{ m}$), V_0 is the initial electron velocity ($=0 \text{ m/s}$), and t is the transit time for an electron to travel from the emission surface to collector. From the above equation, t is calculated to be 0.04 ns. So the delay time for ferroelectric emission should be very short. The major fraction of the delay time would mainly be determined by the repulsive field build up time, which is related to domain switching dynamics, from Fig. 10, it is $\approx 40 \text{ ns}$.

From Eq. (1), we know that the electric field E_g in the triple gaps of PZT EC-64 is $\approx 10^9 \text{ V/m}$. Under this high field, classic field emission occurs, i.e., electrons from the lattice overcome the high surface potential, which then leads to plasma emission. Comparatively the electric field on the ferroelectric surface induced by fast polarization switching is $\approx 10^7 \text{ V/m}$. Although it is two orders of magnitude lower than E_g , it is not unreasonable to expect that mixed mode emission occurs. Since ferroelectric emission has a different emission mechanism, i.e., self-emission, and the emitted electrons are thought to originate from the surface or right below the surface, it is likely that only a very low surface potential needs to be overcome. This might be the reason that both true ferroelectric emission and plasma emission are observed simultaneously in this experiment. However, one should note again that the strong plasma emission described in Refs. 13, 15, and 24, a high positive extraction field was applied to the electron collector. In our experiments (Figs. 4 and 10) no extraction field was applied. Thus this lowered the plasma electron emission current density.

There is still no direct experimental evidence showing that the electrons are emitted from the bare surface of the ferroelectric during ferroelectric emission. However, SEM micrographs of the emission surface before and after emission studies show evidence of microstructural changes on the bare ferroelectric surface.²⁵

IV. CONCLUSIONS

Electron emission from PZT studied under our experimental techniques is a mixed type electron emission process, i.e., both true ferroelectric emission and plasma emission existed simultaneously.

Plasma emission and ferroelectric emission have quite different emission characteristics. For plasma emission, inconsistency and an apparent delay time between electron emission and driving pulse are typical. In addition, a positive ion current was observed. Strong electrode erosion could be expected. Comparatively, ferroelectric emission is a relatively stable self-emission process, and exhibits no apparent delay time. No positive ion current existed.

The relationship between switching and emission current of ferroelectric sample measured simultaneously gives a clearer path to see if ferroelectric emission exists, and to determine the emission efficiency and capability. Thus it can give us the direction to find a suitable ferroelectric material for emitter applications.

ACKNOWLEDGMENTS

This research is sponsored by the DOE through Allied-Signal FM & TC under Contract No. 052G101867. The suggestions from H. Riege (CERN), H. Gundel (CERN), and G. Rosenman (Tel-Aviv.) are deeply appreciated. Work also performed by Lawrence Livermore National Laboratory under Contract No. W-7405-Eng-48.

- ¹H. Riege, *Le Vide les Couches Minces* (suppl. issue) **275**, 398 (1995).
- ²S. E. Sampayan, W. J. Orvis, G. J. Caporaso, and T. F. Wieskamp, US Patent No. 5,508,590 (1996).
- ³O. H. Auciello and G. E. McGuire, US Patent No. 5,453,661 (1995).
- ⁴H. Gundel, *Integr. Ferroelectr.* **5**, 211 (1994).
- ⁵J. Asano, T. Imai, M. Okuyama, and Y. Hamakawa, *Jpn. J. Appl. Phys.*, Part 1 **31**, 3098 (1992).
- ⁶R. Le Bihan, S. F. Liateni, and D. Averty, *Le Vide les Couches Minces* (suppl. issue) **275**, 562 (1995).
- ⁷H. Gundel, H. Riege, and E. J. N. Wilson, *Nucl. Instrum. Methods Phys. Res. A* **280**, 1 (1989).
- ⁸R. C. Miller and A. Savage, *J. Appl. Phys.* **31**, 662 (1960).
- ⁹G. Rosenman and I. Rez, *J. Appl. Phys.* **73**, 1904 (1993).
- ¹⁰H. Gundel, J. Handerek, H. Riege, and E. J. N. Wilson, *Ferroelectrics* **110**, 183 (1990).
- ¹¹H. Gundel, H. Riege, and E. J. N. Wilson, *Ferroelectrics* **100**, 1 (1989).
- ¹²W. M. Zhang, W. Huebner, and G. D. Waddill, *Ferroelectrics* (submitted).
- ¹³D. Shur, G. Rosenman, Y. E. Krask, and V. D. Kugel, *J. Appl. Phys.* **79**, 3669 (1996).
- ¹⁴G. Pleyber, K. Biedrzycki, and R. Le Bihan, *Ferroelectrics* **141**, 125 (1995).
- ¹⁵G. A. Mesyats, *IEEE Trans. Dielectr. Electr. Insul.* **2**, 272 (1995).
- ¹⁶H. Gundel, J. Handerek, and H. Riege, *J. Appl. Phys.* **69**, 975 (1991).
- ¹⁷H. Riege (private communication).
- ¹⁸W. M. Zhang, W. Huebner, S. E. Sampayan, and M. L. Krogh, *J. Am. Ceram. Soc.* (submitted).
- ¹⁹S. E. Sampayan, G. J. Caporiso, W. J. Orvis, and T. F. Wieskamp, UCRL-JC-120507 Preprint, LLNL, 1995 (unpublished).
- ²⁰W. M. Zhang, Ph.D. dissertation, University of Missouri-Rolla, 1997.
- ²¹G. A. Mesyats and D. I. Proskurovsky, *Pulse Electrical Discharge in Vacuum* (Springer, Berlin, 1989), Chap. 6.
- ²²F. F. Cap, *Handbook on Plasma Instabilities* (Academic, London, 1976), Chap. 2.
- ²³J. A. Bittencourt, *Fundamentals of Plasma Physics* (Pergamon, Oxford, 1986), Chap. 1.
- ²⁴M. J. Kofoid, *AIEE Trans.* **79**, 999 (1960).
- ²⁵W. M. Zhang and W. Huebner, *J. Appl. Phys.* (to be published).
- ²⁶G. D. Waddill (private communication).
- ²⁷H. Gundel, *Science and Technology of Electroceramic Thin Films*, edited by O. Auciello and R. Waser (Kluwer Academic, Netherlands, 1995), p. 345.
- ²⁸M. E. Lines and A. M. Glass, *Principles and Applications of Ferroelectrics and Related Materials* (Clarendon, Oxford, 1977), Chap. 4.